# Total cross sections for electron scattering from He and Ne at very low energies

K. Shigemura,[1] M. Kitajima,[1,*] M. Kurokawa,[1] K. Toyoshima,[1] T. Odagiri,[1,†] A. Suga,[2] H. Kato,[2] M. Hoshino,[2] H. Tanaka,[2] and K. Ito[3]

[1]*Department of Chemistry, Tokyo Institute of Technology, Tokyo 152-8551, Japan*

[2]*Department of Physics, Sophia University, Tokyo 102-8554, Japan*

[3]*Photon Factory, Institute of Materials Structure Science, Tsukuba 305-0801, Japan*

(Received 21 January 2014; published 21 February 2014)

Absolute total cross sections for electron scattering from He and Ne are obtained in the energy range from 20 eV down to below 10 meV with a very narrow electron energy width of 6–8 meV using the threshold-photoelectron source. Total cross sections obtained in the present study generally agree well with those obtained in the previous experiments for both He and Ne above 100 meV, where several experimental works have been reported. Comparison of the present cross sections with the theoretical cross sections which have been regarded as the "standard" cross sections shows very good agreement even at very low energies below 10 meV, which confirms the validity of theoretical cross sections. The scattering lengths for electron scattering from He and Ne are also determined from the present total cross sections using the modified effective range theory. The resonant structures in the total cross sections due to Feshbach resonances of He and Ne are also observed. Analysis of the resonant structure was carried out based on the spin-dependent resonant scattering theory in order to determine the values of natural width of Feshbach resonance of Ne.

DOI: 10.1103/PhysRevA.89.022709 PACS number(s): 34.80.Bm, 52.20.Fs

## I. INTRODUCTION

The scattering of low-energy electrons by rare-gas atoms has been the subject of extensive experimental and theoretical investigations. The cross-section data concerning electron scattering from rare-gas atoms are of great importance in understanding fundamental physics of the electron collisions. Reliable cross-section data are also of crucial importance in applications, such as electron driven processes in phenomena of the earth and planets, radiation chemistry, gaseous discharges, plasmas, and so on [1].

As is the simplest system in the electron-atom collision, in which a significant electron-electron correlation already exists in the initial state of the target atom involved, electron scattering from He provides an ideal testing ground for developing a general method for treating electron scattering from atomic targets. Due to its importance, a number of measurements of absolute total cross sections for low-energy-electron scattering from He have been reported [2–11]. It has been shown that experimental total cross sections for He obtained since the late 1970s agree well within the quoted experimental uncertainties above 1 eV [10,11]. The energy range of the total cross-section measurements have been extended down to 100 meV [5,8], which is about the lower limit of beam experiments using hot-filament electron sources. At lower electron energies, electron-swarm techniques have provided the information of electron scattering from He [12,13]. However, difficulty arises in determining the accurate cross section uniquely by the swarm techniques, since the microscopic properties of electron-atom or electron-molecule collision have to be determined in a complicated unfolding procedure by a self-consistent set of cross sections that will reproduce the macroscopic experimental results such as transport coefficients, drift velocity, or mobility, via solution of energy distribution function [14,15]. Therefore, comparison of electron scattering cross sections measured at very low energies under the single collision condition with those determined from swarm techniques is important [16].

Theoretical calculations of elastic electron scattering from He including both polarization and the electron correlation were carried out by O'Malley *et al*. using *R*-matrix calculations [17] and by Nesbet using a convergence variational method [18]. The cross sections reported by O'Malley *et al*. were given from the theoretical estimates by detailed error analysis of their calculated phase shifts. The cross sections of Nesbet [18] were also the estimated values based on the systematic study of convergence of the phase shifts. Results of both O'Malley *et al*. [17] and Nesbet [18] show very good agreement between each other. Since Nesbet presented the results in a form that allows simple computation to obtain integral and differential cross sections for energies up to 19 eV, the cross-section set computed from the report of Nesbet [18] has often been used as the "standard" cross-section set [16,19,20]. Phase shifts obtained in the later large scale multiconfiguration Hartree-Fock calculation of Saha, which takes into account the dynamic target polarization and electron correlation effect [21,22], also show very good agreement with the estimated ones of O'Malley *et al*. [17] and those of Nesbet [18]. Therefore, cross sections of these theoretical reports have been taken as the references that several works rely on. Since theoretical treatment becomes very difficult due to strong contribution of electron correlation and polarization at very low energies close to the zero energy limit, comparison of experimental and theoretical cross sections at very low energies would be necessary for critical assessment of the theoretical treatment. However, comparisons of these theoretical cross sections with accurate experimental total cross sections at very low energies have not been done up to now due to the lack of the experimental cross sections obtained under the single collision condition at very low energies.

*mkitajim@chem.titech.ac.jp

†Present address: Department of Physics, Sophia University, Tokyo 102-8554, Japan.

 

Neon atom has also been a particularly favorable target for testing collision models, since Ne can be regarded as a relatively light target with ground state represented as a compact closed-shell system. Several total cross sections obtained from the beam experiments generally agree with each other especially below 5 eV [7,9,23,24]. Theoretical cross sections show good agreements to the experimental cross sections [25–30]. However, as is in the case of He, accurate experimental total cross sections obtained under the single collision condition at energies below 100 meV are still missing.

Up to now most of the experimental studies on low-energy electron collisions in the gas phase have been performed with a technique using a hot-filament electron source. However, the low energy limits of the method have been limited to about 100 meV in most cases. Measurements of total cross sections for electron scattering from various molecules at the energies below 100 meV under the single-collision condition have been achieved by Field and Ziesel, with co-workers, making use of a photoelectron source together with high resolution synchrotron radiation as an alternative to the standard technique using a hot-filament electron source [31–33]. However, cross sections for electron scattering from rare-gas atoms at very low energies have not been reported by the group.

Recently we developed a method for producing an electron beam at very low energies down to below 10 meV employing the threshold-photoelectron source [34]. The technique enables one to perform high energy-resolution experiments at very low electron energies by employing the penetrating-field technique together with the threshold photoionization of atoms by the synchrotron radiation. The total cross sections for electron scattering from Ar, Kr, and Xe in the energy range from 20 eV down to below 10 meV were obtained with the technique [34,35]. The scattering lengths for the $e^-$-Ar, -Kr, and -Xe scatterings determined from the obtained cross sections showed significant discrepancies from those obtained in the previous experimental and theoretical studies. It is likely that previous values of the scattering length have been determined with the overestimated cross sections at very low energies below 100 meV, where direct measurements in the single-collision condition have not been reported [35].

In the present paper we report the results of the measurements of total cross sections for electron scattering from He and Ne obtained by the experimental technique employing the threshold-photoelectron source in the energy range from 20 eV down to below 10 meV. Since theoretical cross sections for electron scattering from He and Ne, which have been regarded as the standard cross sections, were only confirmed by swarm derived momentum transfer cross sections at very low energies, critical comparison of the theoretical cross sections with accurate experimental total cross sections obtained under the single collision conditions are of significant importance.

## II. EXPERIMENT

The present measurements were carried out at beamline 20A of the Photon Factory, KEK [36], using an electron scattering apparatus equipped with a threshold-photoelectron source [34]. The setup consists of an electron scattering apparatus and a photoionization cell, a photon-flux monitor, and a microchannel plate (MCP). An overview of the experimental setup is shown in Fig. 1.

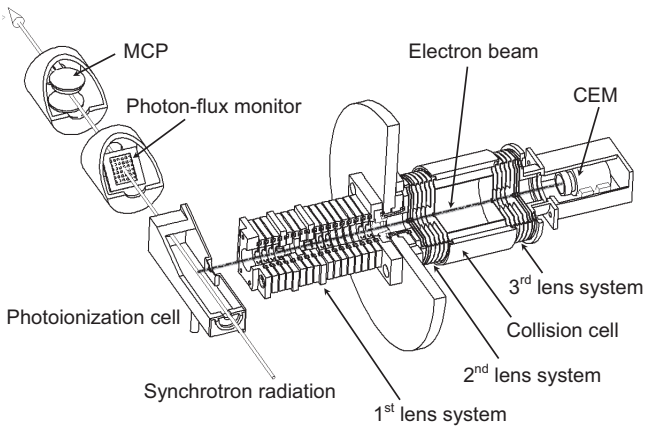


FIG. 1. Overview of the experimental system. The system consists of an electron scattering apparatus with a photoionization cell, a microchannel plate (MCP) to measure photoion yield spectra, and a photon-flux monitor for the monochromatized synchrotron radiation. The monochromatized synchrotron radiation is focused onto the center of the photoionization cell filled with argon atoms for producing photoelectrons. The photoelectrons are collected by the penetrating field from the first lens system and formed into a beam. The electron beam is tuned by the second lens system and focused onto the collision cell filled with target gas. The transmitted electrons are angular discriminated and refocused by the third lens system and detected by a channel electron multiplier (CEM).

The electron scattering apparatus consists of a photoionization cell, three electrostatic lens systems, a collision cell, and a channel electron multiplier. The monochromatized synchrotron radiation tuned just at the first ionization threshold of Ar was focused on the center of the photoionization cell filled with Ar. The threshold photoelectrons produced by the threshold photoionization of Ar atoms are extracted by a weak electrostatic field formed by the penetrating field technique and formed into a beam by the first lens system of the electron scattering apparatus. The penetrating field forms a saddle point in the potential distribution that has the effect of focusing and enhancing the extraction efficiency of photoelectrons of particular energy. By tuning the penetrating field, only very low energy photoelectrons are extracted from the photoionization region and focused onto the lens system, while the energetic photoelectrons rapidly diverge [37]. This effect results in a very narrow energy width of the electron beam from the threshold photoelectron source even if the bandwidth of the ionization photon beam is fairly wide [34]. Doppler broadening of the threshold photoelectrons is very small in the present case. The energy broadening due to the Doppler effect is estimated to be less than 0.1 meV.

The extracted monoenergetic electrons are formed into a beam and fed into the second lens system. The second lens system controls the energy of the electron beam and transmits the beam into the collision cell filled with target gas. The electrons passing through the cell without any collision with the target are angular discriminated and refocused by the third lens system and detected by a channel electron multiplier.

The whole of the photoionization cell and scattering apparatus are placed inside the double $\mu$-metal shields to attenuate the Earth's magnetic field. The stray magnetic field is less than $10^{-7}$ T, which is sufficiently small not to interact with the lowest energy electron in the present experiment. The vacuum chamber is divided into two regions one of which contains the scattering apparatus and the other the photoionization cell, the photon-flux monitor, and the MCP. Both regions are pumped differentially.

The total cross section was obtained by using the attenuation law. The effective path length of the electron in the target gas has been found to be equal to the geometrical length [34]. The transmission of the electron beam was kept above 50% in order to avoid inaccurate measurements for narrow structure known as the line saturation effect [38].

The pressure of target gas was measured by a capacitance manometer kept at a temperature of 318 K. The thermal transpiration correction with the empirical expression developed by Takaishi and Sensui [39] was made in the present measurement. Purity of the gases in the present measurements was 99.9995% for He and 99.999% for Ne.

The effect of the forward scattering, which is the incomplete discrimination against the electrons scattered at small angles with forward direction due to the finite angular resolution, contributes to the measured total cross section in the attenuation method. In the present study, the contributions from the forward scattered electrons of the scattering from He and Ne were estimated by the same manner with our previous work [34]. The CPO computer program [40] was used to calculate the trajectory of the electrons scattered in the collision cell and the theoretical phase shifts reported by Saha [21,22,29] were applied in order to estimate the differential cross sections for the electron scattering from He and Ne. It was found that the contribution from the forward-scattered electron is negligible in the present study.

The energy and the width of the electron beam was estimated by fitting the theoretical cross sections convoluted with a Gaussian function representing the resolution to those measured at around the Feshbach resonances of rare gas atoms following Kurokawa *et al.* [35]. The energy of $19.365 \pm 0.001$ eV [41,42] for the resonance energy of the $He^-$ $(1s2s^2\ ^2S_{1/2})$ resonance and that of $16.1257 \pm 0.0010$ eV [43] for the $Ne^-$ $(2p^53s^2\ ^2P_{3/2})$ resonance were chosen as the reference point. The accuracy of the energy scale of the present measurements was estimated to be $\pm 5$ meV. In case of He, the energy width of the electron beam was estimated by fitting to the $Ar^-$ $(3p^54s^2\ ^2P_{3/2})$ resonance measured under the same experimental condition. The energy widths of the electron beam for total cross-section measurements were estimated to be 8 meV for He and 6 meV for Ne.

## III. RESULTS AND DISCUSSION

### A. Total cross sections for electron scattering from He

The total cross sections for electron scattering from He obtained in the energy range of 6 meV to 20 eV are shown in Figs. 2(a) and 2(b) together with the previous experimental and theoretical cross sections. The numerical values for the selected points are shown in Table I. The overall uncertainty

TABLE I. The values of total cross sections for electron scattering from He and Ne obtained in the present work [here the quoted uncertainties in parentheses refer to the respective last digits, e.g., 3.78(13) means $3.78 \pm 0.13$].

| | $\sigma(E)$ $(10^{-20}$ m$^2)$ | |
|---|---|---|
| Energy (eV) | He | Ne |
| 20.075 | | 3.78(13) |
| 20.029 | 3.09(8) | |
| 19.075 | | 3.69(13) |
| 19.029 | 3.17(8) | |
| 18.075 | | 3.68(13) |
| 18.029 | 3.28(8) | |
| 17.075 | | 3.73(13) |
| 17.029 | 3.37(8) | |
| 16.074 | | 3.61(9) |
| 16.029 | 3.46(8) | |
| 15.075 | | 3.60(13) |
| 15.029 | 3.62(8) | |
| 14.075 | | 3.64(13) |
| 14.029 | 3.74(8) | |
| 13.075 | | 3.56(13) |
| 13.029 | 3.86(8) | |
| 12.075 | | 3.53(13) |
| 12.029 | 4.02(8) | |
| 11.075 | | 3.55(13) |
| 11.029 | 4.17(8) | |
| 10.075 | | 3.44(13) |
| 10.029 | 4.40(8) | |
| 9.075 | | 3.28(13) |
| 9.029 | 4.55(8) | |
| 8.075 | | 3.23(13) |
| 8.029 | 4.74(8) | |
| 7.075 | | 3.21(13) |
| 7.029 | 4.90(8) | |
| 6.075 | | 3.00(13) |
| 6.029 | 5.13(8) | |
| 5.075 | | 2.85(14) |
| 5.029 | 5.38(8) | |
| 4.075 | | 2.61(14) |
| 4.029 | 5.58(8) | |
| 3.075 | | 2.41(14) |
| 3.029 | 5.84(8) | |
| 2.675 | | 2.23(14) |
| 2.429 | 6.00(8) | |
| 2.275 | | 2.18(14) |
| 2.075 | | 1.98(14) |
| 2.029 | 6.04(8) | |
| 1.875 | | 1.96(14) |
| 1.829 | 6.13(8) | |
| 1.675 | | 2.04(14) |
| 1.629 | 6.13(8) | |
| 1.475 | | 1.95(14) |
| 1.429 | 6.14(8) | |
| 1.275 | | 1.69(14) |
| 1.229 | 6.17(8) | |
| 1.075 | | 1.62(14) |
| 1.029 | 6.14(7) | |
| 0.975 | | 1.52(14) |
| 0.909 | 6.11(7) | |
| 0.875 | | 1.50(14) |
| 0.809 | 6.10(7) | |

TABLE I. (*Continued.*)

| | $\sigma(E)$ ($10^{-20}$ m$^2$) | |
|---|---|---|
| Energy (eV) | He | Ne |
| 0.775 | | 1.38(14) |
| 0.709 | 6.06(7) | |
| 0.675 | | 1.27(14) |
| 0.609 | 6.05(7) | |
| 0.575 | | 1.30(14) |
| 0.509 | 6.03(7) | |
| 0.475 | | 1.18(14) |
| 0.409 | 5.98(7) | |
| 0.375 | | 1.09(14) |
| 0.309 | 5.98(7) | |
| 0.275 | | 0.97(7) |
| 0.269 | 5.93(7) | |
| 0.235 | | 0.92(7) |
| 0.229 | 5.94(14) | |
| 0.195 | | 0.86(7) |
| 0.181 | 5.90(14) | |
| 0.175 | | 0.87(7) |
| 0.169 | 5.85(14) | |
| 0.155 | | 0.78(7) |
| 0.149 | 5.86(14) | |
| 0.135 | | 0.73(7) |
| 0.129 | 5.78(14) | |
| 0.115 | | 0.72(7) |
| 0.109 | 5.71(14) | |
| 0.095 | | 0.68(8) |
| 0.089 | 5.77(14) | |
| 0.075 | | 0.54(8) |
| 0.069 | 5.68(14) | |
| 0.067 | | 0.47(8) |
| 0.061 | 5.68(15) | |
| 0.059 | | 0.48(8) |
| 0.054 | 5.69(16) | |
| 0.051 | | 0.46(9) |
| 0.046 | 5.70(16) | |
| 0.043 | | 0.35(10) |
| 0.042 | 5.59(16) | |
| 0.039 | | 0.47(11) |
| 0.038 | 5.63(16) | |
| 0.035 | | 0.45(11) |
| 0.034 | 5.56(16) | |
| 0.031 | | 0.52(12) |
| 0.030 | 5.48(16) | |
| 0.027 | | 0.22(13) |
| 0.026 | 5.54(16) | |
| 0.023 | | 0.32(13) |
| 0.022 | 5.43(17) | |
| 0.020 | 5.41(17) | |
| 0.019 | | 0.34(14) |
| 0.018 | 5.25(17) | |
| 0.016 | 5.16(17) | |
| 0.015 | | 0.27(14) |
| 0.014 | 5.17(17) | |
| 0.012 | 5.31(17) | |
| 0.011 | | 0.27(13) |
| 0.010 | 5.22(17) | |
| 0.008 | 5.16(17) | |
| 0.007 | | 0.25(14) |
| 0.006 | 5.26(17) | |

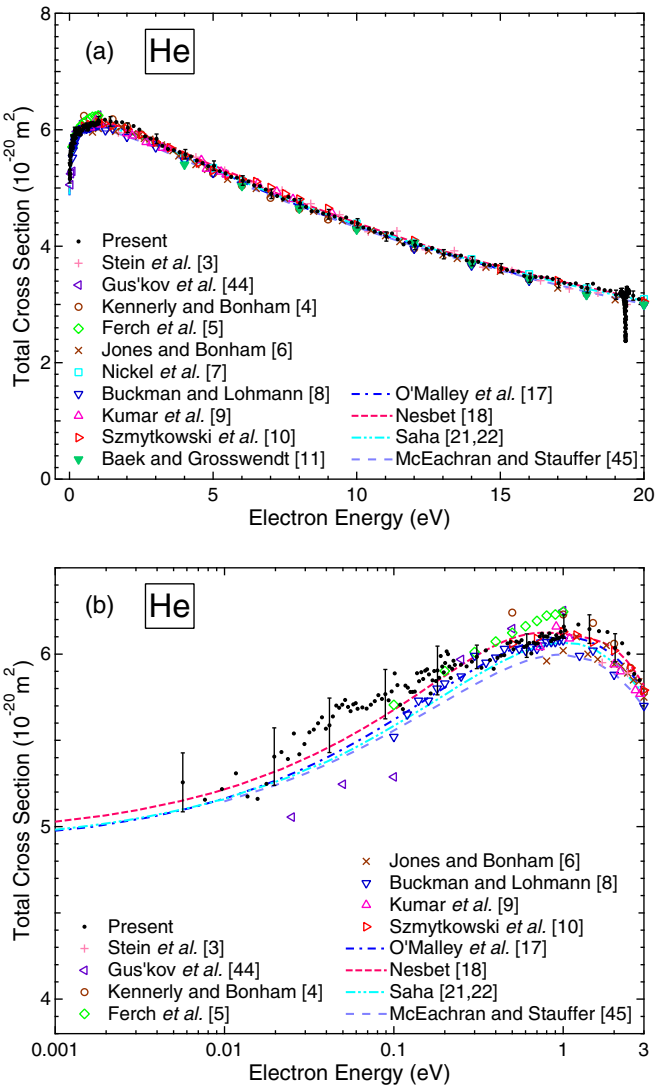


FIG. 2. (Color online) Total cross sections for electron scattering from He (a) in the energy range up to 20 eV, and (b) in the energy range below 3 eV: •, present results; +, Stein *et al.* [3]; ◁, Gus'kov *et al.* [44]; ○, Kennerly and Bonham [4]; ◇, Ferch *et al.* [5]; ×, Jones and Bonham [6]; □, Nickel *et al.* [7]; ▽, Buckman and Lohmann [8]; △, Kumar *et al.* [9]; ▷, Szmytkowski *et al.* [10]; ▼, Baek and Grosswendt [11]; _ . _ . _, O'Malley *et al.* [17]; _ _ _, Nesbet [18]; _ · _ · _ · _, Saha [21,22]; _ _ _, McEachran and Stauffer [45].

in the cross section includes the statistical and systematic error. The lowest energy of experimentally obtained total cross sections for electron scattering from He is extended down to 6 meV in the present work. The cross section rises from 6 meV and shows maximum at around 1 eV. Above 1 eV, the cross section decreases with increasing the energy. The prominent feature at 19.37 eV observed in the present total cross-section curve in Fig. 2(a) is the sharp dip due to the $He^-$ ($1s2s^2\ ^2S_{1/2}$) Feshbach resonance.

In general, present results agree well with the previously reported experimental cross sections. Among the previous experimental cross sections, the present results agree very well with the results of Nickel *et al.* [7] above 4 eV. At low energies, present cross sections agree with those of Buckman

and Lohmann [8] in the energy range from 1 eV down to 200 meV within the experimental errors. Below 200 meV, the present results agree well with the cross sections of Ferch *et al.* [5], which shows slightly larger cross sections compared to those of Buckman and Lohmann [8], though both results agree with each other within the experimental errors. At energies below 100 meV, Gus'kov *et al.* have reported experimental total cross sections down to 25 meV [44]. The values reported by Gus'kov *et al.* in the energy region below 100 meV are somewhat smaller compared to the present results.

In Figs. 2(a) and 2(b) theoretical integral elastic cross sections of *R*-matrix calculations by O'Malley *et al.* [17] and those of convergence variational method by Nesbet [18] together with the results of multiconfiguration Hartree-Fock calculation by Saha [21,22] are also shown for comparison. Since only the elastic scattering channel is open below the first excited state of He* ($2s\,^3S$) at 19.82 eV in the $e^-$-He scattering, present total cross sections obtained below 19.82 eV represents the integral elastic cross sections. The present cross sections agree very well with these theoretical cross sections in the entire energy range below 19.82 eV except for the resonance structure. The differences of the cross-section values between present results and these theoretical results are less than 5% and all of the three theoretical results lie within the present experimental errors even at the very low energy of 6 meV. The present results prove the validity of the theoretical cross sections of He which have been the standard cross sections at very low energy region below 100 meV, where theoretical treatment becomes very difficult due to strong contribution of electron correlation and polarization.

Results of McEachran and Stauffer [45] using the polarized-orbital calculation with dipole adiabatic-exchange approximation which includes dynamic distortion effects are also shown in Figs. 2(a) and 2(b). Their polarized-orbital calculation including dynamic distortion effects [45] show good agreement with the present cross sections. It should be noted that the results of earlier calculation of McEachran and Stauffer using polarized-orbital calculation with dipole adiabatic-exchange approximation but neglecting the dynamic term [25] do not agree with the present cross sections.

The scattering length for electron scattering from He was derived using the modified effective range theory (MERT) [46,47] in the present study. MERT gives analytical expressions for the scattering phase shifts as a function of wave number of electron $k$ expressed in the form of expansion of power series in $k$ using the dipole polarizability of the target atom. As was pointed out by Buckman and Lohmann, it is not possible to unambiguously determine both the $s$- and the $p$-wave phase shifts, due to the lack of a strong energy dependence of the cross section in case of He [8]. Here we applied MERT fit by fixing the $p$- and $d$-wave phase shifts using the calculated values of Nesbet [18] and employing the $s$-wave phase shift in the standard four parameter MERT (MERT4) [47–50] as

$$\tan\delta_0(k) = -Ak\left[1 + \frac{4\alpha_d k^2}{3a_0}\ln(ka_0)\right] - \frac{\pi\alpha_d k^2}{3a_0} + Dk^3 + Fk^4, \quad (1)$$

TABLE II. Comparison of scattering length for He obtained from present MERT analysis with those obtained in previous studies.

| | Scattering length (units of $a_0$) |
|---|---|
| Present work | 1.194(6) |
| Ferch *et al.* [5] | 1.195 |
| Buckman and Lohmann [8] | 1.16 |
| Fedus *et al.* [51][a] | 1.186 |
| Crompton *et al.* [13] | 1.19 |
| O'Malley *et al.* [17] | 1.177 |
| Nesbet [18] | 1.1835 |
| Saha [22] | 1.1784 |

[a]An alternative MERT fit to the cross sections of Buckman and Lohmann [8].

where $\alpha_d$ is the dipole polarizability of the atom, $A$ is the scattering length, and $D$ and $F$ are additional fitting parameters. The present fit in the energy range up to 0.3 eV gave scattering length of $1.194 \pm 0.006\ a_0$. Comparison of the values of scattering length obtained in the present MERT analysis with those reported in the previous studies are made in Table II. In contrast to the case of Ar, Kr, and Xe [35], present scattering length for He agrees well with the values obtained in the previous studies. Present scattering length agree very well with the results of Ferch *et al.* obtained by the single collision experiment [5]. Buckman and Lohmann reported slightly smaller scattering length compared to the present value [8]. However, recent reanalysis of their data by Fedus *et al.* using an alternative MERT fit results in very close value to the present one [51]. Here we also note that the agreement of the present scattering length with the results of the swarm experiment of Crompton [13] is very good, which indicates that the present total cross sections are consistent to the swarm driven momentum transfer cross sections of Crompton at very low energies.

### B. Total cross sections for electron scattering from Ne

Figures 3(a) and 3(b) show the total cross sections for electron scattering from Ne obtained in the energy range of 7 meV to 20 eV in the present experiment together with the previous experimental and theoretical cross sections. The numerical values for the selected points are also shown in Table I. Magnitude of the cross sections decreases with decreasing the electron energy below 20 eV and approaches to a very small value at the lowest energy. Very sharp structures due to the $Ne^-$ ($2p^5 3s^2\ ^2P_{3/2}$) and the $Ne^-$ ($2p^5 3s^2\ ^2P_{1/2}$) Feshbach resonance are seen at about 16 eV.

The present results agree very well with previous experimental total cross sections of Nickel *et al.* [7], Szmytkowski *et al.* [10], and Baek and Grosswendt [11] in the energy region from 20 down to 4 eV. At lower energies, our data agree very well with results of Gulley *et al.* [24] down to 100 meV. The cross sections of Gus'kov *et al.* [44] show large discrepancy from the present results.

Among the theoretical cross sections for electron scattering from Ne, the elastic integral cross sections of McEachran and Stauffer [27], and those of Saha [28,29], are shown in Figs. 3(a) and 3(b) for the comparison. The theoretical total cross sections

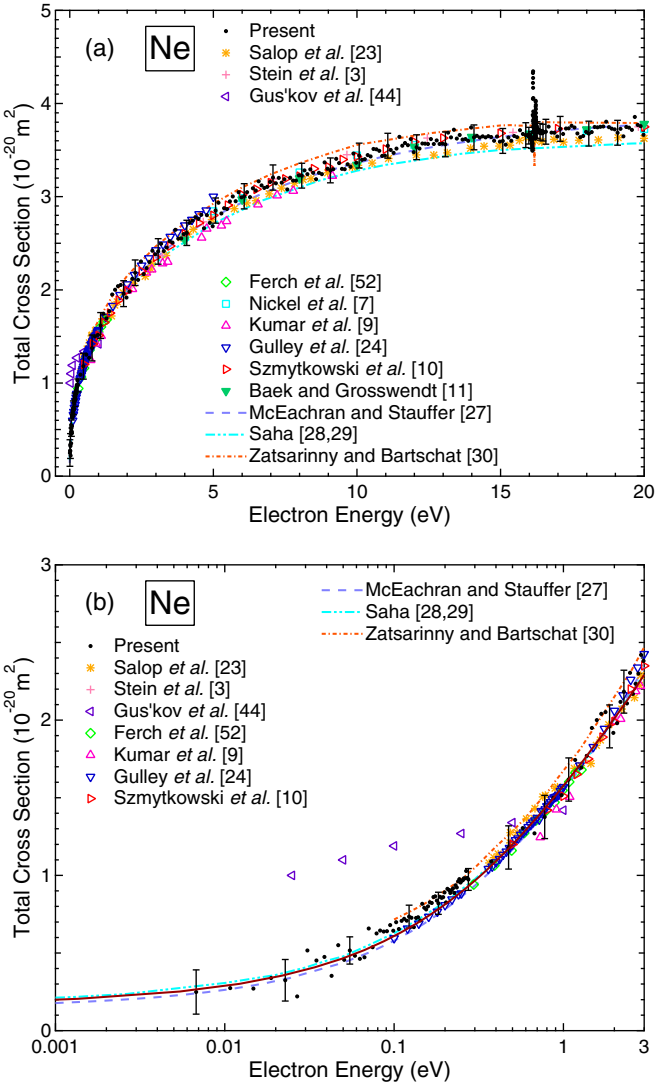


FIG. 3. (Color online) Total cross sections for electron scattering from Ne (a) in the energy range up to 20 eV, and (b) in the energy range below 3 eV: •, present results; ✳, Salop and Nakano [23]; +, Stein *et al.* [3]; ◁, Gus'kov *et al.* [44]; ◇, Ferch *et al.* [52]; □, Nickel *et al.* [7]; △, Kumar *et al.* [9]; ▽, Gulley *et al.* [24]; ▷, Szmytkowski *et al.* [10]; ▼, Baek and Grosswendt [11]; _ _ _, McEachran and Stauffer [27]; _ . _ . _, Saha [28,29]; _ . . _ . . _, Zatsarinny and Bartschat [30].

of the recent large scale $R$-matrix calculation by Zatsarinny and Bartschat [30] are also shown in Figs. 3(a) and 3(b). The cross sections obtained in the multiconfiguration Hartree-Fock calculation by Saha [28,29] show very good agreement with the present results at energies below 3 eV as is the case for He. Although the cross sections of Saha show slightly smaller cross sections at higher energies, agreement with the present results at the very low energies down to 7 meV is excellent. This shows the capability of the multiconfiguration Hartree-Fock calculation for treating the scattering problem at very low energies not only for He but also for Ne.

The results of McEachran and Stauffer [27] using the polarized-orbital calculation with dipole adiabatic-exchange approximation show very good agreement with the present results. The theoretical model employed in their calculation was basically the same approach used in the calculation of He by the same authors which neglect the dynamic distortion effects [25] except for the scaling of the polarization potential. In case of He, including the effects of the dynamic distortion in the polarized-orbital calculation, McEachran and Stauffer obtained much improved results [45] compared to their earlier calculation which neglects the dynamic term [25]. However, their attempt to include the effects of the dynamic distortion in the polarized-orbital calculation for Ne have failed due to the difficulties in obtaining the accurate polarization for Ne in their approach [53].

TABLE III. Comparison of scattering length for Ne obtained from present MERT analysis with those obtained in previous studies.

| | Scattering length (units of $a_0$) |
|---|---|
| Present work | 0.206(19) |
| Buckman and Mitroy [50] | 0.206 |
| O'Malley and Crompton [48] | 0.2135 |
| McEachran and Stauffer [27] | 0.2012 |
| Saha [29] | 0.2218 |

The recent large-scale $R$-matrix-with-pseudostates calculations by Zatsarinny and Bartschat [30] show slightly larger cross sections compared to the present results in the energy range below 20 eV. Theoretical treatment of Zatsarinny and Bartschat handles excitation and ionization processes as well as elastic scattering, in contrast to other calculations which were designed to treat only the elastic scattering. Their calculation also has the capability of including influence of the strong $Ne^-$ $(2p^5 3s^2\ ^2P_{3/2,1/2})$ Feshbach resonances just above 16 eV. Although the energy range of their calculation has been limited down to 100 meV, it is interesting to see how the recent large-scale calculation works at very low energies.

Scattering length of $0.206 \pm 0.019\ a_0$ were obtained in the MERT fit to the present cross sections of Ne in the energy range up to 0.3 eV. As in the case of He, we applied MERT fit by fixing the $p$- and $d$-wave phase shifts using the calculated values of Saha [29] and employing the $s$-wave phase shift of MERT4 form of Eq. (1). Comparison of the values of scattering length obtained in the present MERT analysis with those reported in the previous studies are made in Table III. The present value agrees well with those obtained in the previous studies for both theoretical and experimental works including the swarm results of O'Malley and Crompton [48]. This confirms the momentum transfer cross sections of O'Malley and Crompton in the very low energy region.

### C. Total cross sections for electron scattering from He and Ne at around the Feshbach resonances

In the present study a prominent feature due to the $He^-$ $(1s2s^2\ ^2S_{1/2})$ Feshbach resonance was observed in the total cross-section curve. Since the pioneering observation of the $He^-$ $(1s2s^2\ ^2S_{1/2})$ Feshbach resonance by Schulz [54], several experimental and theoretical work have been carried out to determine its energy position, resonance width, and the values of scattering phase shifts of atomic negative-ion resonances (see for instance the review by Buckman and Clark [24]). However, structure due to the Feshbach resonance in the total

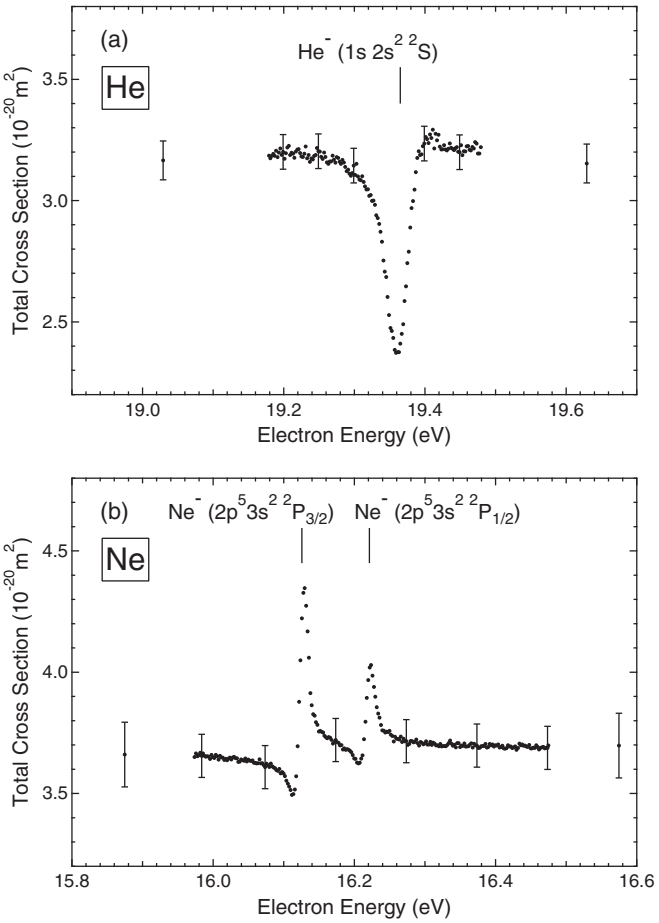


FIG. 4. Total cross sections for electron scattering from He and Ne at around the Feshbach resonances. Vertical bars represent the energy position corresponding to the Feshbach resonances. (a) Cross sections for He at around the $He^-$ $(1s2s^2\ ^2S_{1/2})$ resonance. (b) Cross sections for Ne at around the $Ne^-$ $(2p^53s^2\ ^2P_{3/2})$ and the $Ne^-$ $(2p^53s^2\ ^2P_{1/2})$ resonances.

cross-section curve of He have not been reported except for the old measurement of Golden and Bandel [2]. Figure 4(a) shows the structure of the $He^-$ $(1s2s^2\ ^2S_{1/2})$ Feshbach resonance on the total cross-section curve obtained in the present work. An asymmetric dip-type Fano profile is clearly seen in Fig. 4(a).

In the case of Ne, double peak structure due to the $Ne^-$ $(2p^53s^2\ ^2P_{3/2})$ and the $Ne^-$ $(2p^53s^2\ ^2P_{1/2})$ Feshbach resonances were seen as shown in Fig. 4(b). These resonances have also been observed by Schulz [54]. Simpson and Fano were also the earliest to observe these resonances and classified these states [55]. Unlike the resonance of He, the ion core of Ne resonance having $2p^{-1}$ electron configuration splits into the $J = 3/2$ state and the $J = 1/2$ state due to the spin-orbit coupling which differs in the energy by 97 meV. The splitting of the two resonances determined by the recent high resolution differential cross-section measurements using laser photoelectron by Bömmels *et al.* [43] is 95.5 meV. Bömmels *et al.* also determined the energy position and resonance width of these resonances precisely [43]. The structures of the $Ne^-$ $(2p^53s^2\ ^2P_{3/2})$ and the $Ne^-$ $(2p^53s^2\ ^2P_{1/2})$ Feshbach resonances observed in the present work show asymmetric Fano profiles with almost the same shapes with each other as shown in Fig. 4(b). The intensity of the resonant structure of the $^2P_{3/2}$ resonance is twice as that of the $^2P_{1/2}$ resonance as is expected from the statistical ratio.

The width of the resonance which only decays into the elastic scattering channel, can be determined through the partial-wave analysis with spin-orbit coupling [55,56]. The partial wave analysis with spin-orbit coupling gives integral cross sections for elastic scattering close to the resonances as

$$\sigma(E) = \frac{\pi}{k^2}\left\{8\sin^2\left[\delta_1^{0+}(E) - \cot^{-1}\frac{E - E_{3/2}}{\Gamma_{3/2}/2}\right] + 4\sin^2\left[\delta_1^{0-}(E) - \cot^{-1}\frac{E - E_{1/2}}{\Gamma_{1/2}/2}\right]\right\} + \frac{\pi}{k^2}\sum_{l\neq 1}\left\{4(l+1)\sin^2\delta_l^{0+}(E) + 4l\sin^2\delta_l^{0-}(E)\right\}, \tag{2}$$

where $k$ is the wave number of the electron related to the collision energy $E$, $\delta_l^{0+}(E)$ and $\delta_l^{0-}(E)$ are the potential (nonresonant) scattering phase shifts in the partial wave with total electronic angular momenta of $j^+ = l + 1/2$ and $j^- = l - 1/2$ ($l = 1$ for the resonance of Ne), respectively, $\Gamma_{3/2}$ and $\Gamma_{1/2}$ are the half-width (natural width) of the $J = 3/2$ and the $J = 1/2$ resonances, and $E_{3/2}$ and $E_{1/2}$ are the corresponding resonance energies. The nonresonant scattering phase shifts $\delta_l^{0+}(E)$ and $\delta_l^{0-}(E)$ vary only slowly with electron energy. Following our previous work [35], the width of the $Ne^-$ $(2p^53s^2\ ^2P_{3/2})$ and the $Ne^-$ $(2p^53s^2\ ^2P_{1/2})$ resonances were estimated from the present total cross-section curve. Since spin-orbit splitting is rather small for Ne, we assumed that nonresonant phase shifts $\delta_1^{0+}$ and $\delta_1^{0-}$ are the same, i.e., $\delta_1^{0+} = \delta_1^{0-} \equiv \delta_1^{0\pm}$. Both resonance widths $\Gamma_{3/2}$ and $\Gamma_{1/2}$ are also assumed to be the same, i.e., $\Gamma_{3/2} = \Gamma_{1/2} \equiv \Gamma$, in the present fit. In the present work, the resonance width $\Gamma$, the energy width of the electron beam, and nonresonant phase shift for $l = 1$ partial wave $\delta_1^{0\pm}$ were the fitting parameters. The results of the nonresonant phase shift $\delta_1^{0\pm}$ and resonance width $\Gamma$ obtained in the present analysis are shown in Table IV together with those reported in the previous work.

TABLE IV. Comparison of the resonance widths $\Gamma$ of the $Ne^-$ $(2p^53s^2\ ^2P_{3/2,1/2})$ resonances and the nonresonant phase shift of $l = 1$ partial wave phase shift $\delta_1^{0\pm}$.

| Reference | $\delta_1^{0\pm}$ (rad) | $\Gamma$ (meV) |
|---|---|---|
| Present work | −0.362 | 1.17(7) |
| Simpson and Fano (1963) [55] | ∼−0.26 | >1 |
| Andrick and Ehrhardt (1966) [57] | −0.349 | |
| Roy *et al.* (1975) [58] | | 1.4–1.8 |
| Brunt *et al.* (1977) [59] | | 1.3(4) |
| McEachran and Stauffer (1985) [27] | −0.361 | |
| Saha (1989) [28] | −0.339 | |
| Dubé *et al.* (1993) [60] | −0.349 | 1.30(15) |
| Bömmels *et al.* (2005) (Expt.) [43] | −0.357 | 1.27(7) |
| Bömmels *et al.* (2005) (Theor.) [43] | −0.363 | 1.52 |

The present resonance width show a slightly small value compared to those obtained in the previous work. Among the experimentally obtained values of width Γ, the present value is close to the recent value of Bömmels *et al.* [43]. The experimental value of Bömmels *et al.* was obtained by the phase shift analysis of the extremely high-resolution differential-cross-section measurements using a laser photoelectron source and a supersonic atomic beam as a target. The small difference may be the results of different values of nonresonant phase shift for $l = 1$ partial wave derived in both studies. Although the experimental resolution of the present work is lower due to the Doppler broadening in a static gas target, present analysis has an advantage that the fit can be easily carried out without suffering from choosing the reliable phase shifts for nonresonant partial waves. The present nonresonant phase shift is very close to the theoretically obtained value in the work of Bömmels *et al.* The value also is in good agreement with the theoretical phase shift of McEachran and Stauffer [27] which gives the elastic integral cross sections that agree with the present total cross sections other than the resonant structure.

## IV. CONCLUSIONS

The absolute total cross sections for electron scattering from He in the energy range of 6 meV to 20 eV were obtained with an electron energy width of 8 meV using the threshold-photoelectron source. The present total cross sections generally agree well with those obtained in the previous experiments above 100 meV. Comparisons of the present cross sections with the theoretically obtained standard cross sections of He by O'Malley *et al.* [17] and Nesbet [18], and Saha [21,22] show very good agreement in the electron energy range down to the lowest energy of 6 meV. The absolute total cross sections for electron scattering from Ne were also obtained in the energy range of 7 meV to 20 eV with an electron energy width of 6 meV. The present cross sections of Ne agree very well with the theoretical cross sections of McEachran and Stauffer [27], and those of Saha [28,29] in the very low energy range below 100 meV. It has been shown from the present results that the modern theoretical treatment for the electron scattering from simple closed-shell targets such as He and Ne is valid even at the very low energies. The present results also proved the reliability of the theoretically obtained standard cross sections.

Scattering lengths for the $e^-$-He and the $e^-$-Ne scatterings were also determined using the modified effective range theory (MERT). In contrast to the case of heavier rare gas atoms, such as Ar, Kr, and Xe, where significant discrepancies were found between the scattering lengths derived from MERT analysis to our total cross sections and those reported in previous studies [35], present values of scattering lengths for He and Ne agree well with the values obtained in the previous experimental and theoretical studies. It is also noted that present results also support the swarm derived momentum transfer cross sections of Crompton [13] for He and those of O'Malley and Crompton [48] for Ne at very low energies.

A prominent feature with an asymmetric dip structure due to the $He^-$ $(1s2s^2\ ^2S_{1/2})$ Feshbach resonance was observed in the total cross-section curve of He. Very sharp peaks with asymmetric Fano profiles with almost the same shapes with each other due to the $Ne^-$ $(2p^53s^2\ ^2P_{3/2})$ and the $Ne^-$ $(2p^53s^2\ ^2P_{1/2})$ Feshbach resonances were observed in the total cross-section curve of Ne. The widths of the $Ne^-$ $(2p^53s^2\ ^2P_{3/2})$ and the $Ne^-$ $(2p^53s^2\ ^2P_{1/2})$ resonances and the nonresonant scattering phase shift for the $l = 1$ partial wave at around the resonance region were obtained from the partial wave analysis of the measured total cross sections. The present width is slightly narrower compared with those obtained by the recent study based on the differential-cross-section measurement at very high resolution [43]. The obtained nonresonant scattering phase shift for the $l = 1$ partial wave was very close to theoretically obtained value in the work of Bömmels *et al.* [43] and that by the calculation of McEachran and Stauffer [27].

## ACKNOWLEDGMENTS

This work was supported by the Grant-in-Aid for Scientific Research (C) (Grants No. 20540387 and No. 24540423) the Japan Society for the Promotion of Science, and a Cooperative Research Grant from National Institute for Fusion Science, Japan (Grants No. NIFS06KYAM010 and No. NIFS12KEMF040). This work has been carried out under the approval of Photon Factory Program Advisory Committee for proposals No. 2010G603 and No. 2012G516.

[1] Y. Hatano, Y. Katsumura, and A. Mozumder (eds.), *Charged Particle and Photon Interactions With Matter* (CRC, Boca Raton, FL, 2011).
[2] D. E. Golden and H. W. Bandel, Phys. Rev. **138**, A14 (1965).
[3] T. S. Stein, W. E. Kauppila, V. Pol, J. H. Smart, and G. Jesion, Phys. Rev. A **17**, 1600 (1978).
[4] R. E. Kennerly and R. A. Bonham, Phys. Rev. A **17**, 1844 (1978).
[5] J. Ferch, W. Raith, and K. Schröder, J. Phys. B **13**, 1481 (1980).
[6] R. K. Jones and R. A. Bonham, Aust. J. Phys. **35**, 559 (1982).
[7] J. C. Nickel, K. Imre, D. F. Register, L. Vuskovic, and S. Trajmar, J. Phys. B **18**, 125 (1985).
[8] S. J. Buckman and B. Lohmann, J. Phys. B **19**, 2547 (1986).
[9] V. Kumar, E. Krishnakumar, and K. P. Subramanian, J. Phys. B **20**, 2899 (1987).
[10] C. Szmytkowski, K. Maciąg, and G. Karwasz, Phys. Scr. **54**, 271 (1996).
[11] W. Y. Baek and B. Grosswendt, J. Phys. B **36**, 731 (2003).
[12] L. S. Frost and A. Phelps, Phys. Rev. **136**, A1538 (1964).
[13] R. W. Crompton, M. T. Elford, and A. G. Robertson, Aust. J. Phys. **23**, 667 (1970).
[14] B. Schmidt, K. Berkhan, B. Götz, and M. Müller, Phys. Scr. T **53**, 30 (1994).
[15] A. L. Petrović, S. Dujko, D. Marić, G. Malović, Ž. Nikitović, O. Šašić, J. Jovanović, V. Stojanović, and M. Radmilović-Radenović, J. Phys. D **42**, 194002 (2009).
[16] S. J. Buckman and M. J. Brunger, Aust. J. Phys. **50**, 483 (1997).
[17] T. F. O'Malley, P. G. Burke, and K. A. Berrington, J. Phys. B **12**, 953 (1979).

[18] R. K. Nesbet, Phys. Rev. A **20**, 58 (1979).
[19] L. Boesten and H. Tanaka, At. Data Nucl. Data **52**, 25 (1992).
[20] J. Mitroy, J. Y. Zhang, and K. Varga, Phys. Rev. Lett. **101**, 123201 (2008).
[21] H. P. Saha, Phys. Rev. A **40**, 2976 (1989).
[22] H. P. Saha, Phys. Rev. A **48**, 1163 (1993).
[23] A. Salop and H. H. Nakano, Phys. Rev. A **2**, 127 (1970).
[24] R. J. Gulley, D. T. Alle, M. J. Brennan, M. J. Brunger, and S. J. Buckman, J. Phys. B **27**, 2593 (1994).
[25] R. P. McEachran and A. D. Stauffer, J. Phys. B **16**, 4023 (1983).
[26] W. C. Fon, K. A. Berrington, and A. Hibbert, J. Phys. B **17**, 3279 (1984).
[27] R. P. McEachran and A. D. Stauffer, Phys. Lett. A **107**, 397 (1985).
[28] H. P. Saha, Phys. Rev. A **39**, 5048 (1989).
[29] H. P. Saha, Phys. Rev. Lett. **65**, 2003 (1990).
[30] O. Zatsarinny and K. Bartschat, Phys. Rev. A **85**, 062710 (2012).
[31] D. Field, J. P. Ziesel, P. M. Guyon, and T. R. Govers, J. Phys. B **17**, 4565 (1984).
[32] D. Field, D. W. Knight, G. Mrotzek, J. Randell, S. L. Lunt, J. B. Ozenne, and J. P. Ziesel, Meas. Sci. Technol. **2**, 757 (1991).
[33] S. V. Hoffmann, S. L. Lunt, N. C. Jones, D. Field, and J.-P. Ziesel, Rev. Sci. Instrum. **73**, 4157 (2002).
[34] M. Kurokawa, M. Kitajima, K. Toyoshima, T. Odagiri, H. Kato, H. Kawahara, M. Hoshino, H. Tanaka, and K. Ito, Phys. Rev. A **82**, 062707 (2010).
[35] M. Kurokawa, M. Kitajima, K. Toyoshima, T. Kishino, T. Odagiri, H. Kato, M. Hoshino, H. Tanaka, and K. Ito, Phys. Rev. A **84**, 062717 (2011).
[36] K. Ito, Y. Morioka, M. Ukai, N. Kouchi, Y. Hatano, and T. Hayaishi, Rev. Sci. Instrum. **66**, 2119 (1995).
[37] S. Cvejanović and F. H. Read, J. Phys. B **7**, 1180 (1974).
[38] W. F. Chan, G. Cooper, and C. E. Brion, Phys. Rev. A **44**, 186 (1991).
[39] T. Takaisi and Y. Sensui, Trans. Faraday Soc. **59**, 2503 (1963).
[40] F. H. Read and N. J. Bowring, Charged Particle Optics programs, http://www.electronoptics.com
[41] A. Gopalan, J. Bömmels, S. Götte, A. Landwehr, K. Franz, M.-W. Ruf, H. Hotop, and K. Bartschat, Eur. Phys. J. D **22**, 17 (2003).
[42] K. Franz, T. H. Hoffmann, J. Bömmels, A. Gopalan, G. Sauter, W. Meyer, M. Allan, M.-W. Ruf, and H. Hotop, Phys. Rev. A **78**, 012712 (2008).
[43] J. Bömmels, K. Franz, T. H. Höffmann, A. Gopalan, O. Zatsarinny, K. Bartschat, M.-W. Ruf, and H. Hotop, Phys. Rev. A **71**, 012704 (2005).
[44] Yu. K. Gus'kov, R. V. Savvov, and V. A. Slobodyanyuk, Sov. Phys.-Tech. Phys. **23**, 167 (1978).
[45] R. P. McEachran and A. D. Stauffer, J. Phys. B **20**, 3483 (1987).
[46] T. F. O'Malley, L. Rosenberg, and L. Spruch, Phys. Rev. **125**, 1300 (1962).
[47] T. F. O'Malley, Phys. Rev. **130**, 1020 (1963).
[48] T. F. O'Malley and R. W. Crompton, J. Phys. B **13**, 3451 (1980).
[49] J. Ferch, B. Granitza, C. Masche, and W. Raith, J. Phys. B **18**, 967 (1985).
[50] S. J. Buckman and J. Mitroy, J. Phys. B **22**, 1365 (1989).
[51] K. Fedus, G. P. Karwasz, and Z. Idziaszek, Phys. Rev. A **88**, 012704 (2013).
[52] J. Ferch (1985), unpublished, the cross-section data reported in Ref. [27] are cited here.
[53] D. J. R. Mimnagh, R. P. McEachran, and A. D. Stauffer, J. Phys. B **26**, 1727 (1993).
[54] G. J. Schulz, Phys. Rev. Lett. **10**, 104 (1963).
[55] J. A. Simpson and U. Fano, Phys. Rev. Lett. **11**, 158 (1963).
[56] T. Suzuki, H. Tanaka, M. Saito, and H. Igawa, J. Phys. Soc. Jpn. **39**, 195 (1978).
[57] D. Andrick and H. Ehrhardt, Z. Phys. **192**, 99 (1966).
[58] D. Roy, A. Delage, and J.-D. Carette, J. Phys. E **8**, 109 (1984).
[59] J. N. H. Brunt, G. C. King, and F. H. Read, J. Phys. B **10**, 1289 (1977).
[60] D. Dubé, D. Tremblay, and D. Roy, Phys. Rev. A **47**, 2893 (1993).